

Protocol Design Issues in Underwater Acoustic Networks

Paolo Casari, Michele Zorzi

Department of Information Engineering, University of Padova, Italy

Abstract

In this paper we discuss issues related to the design of underwater acoustic network protocols which are tailored around, and leverage on, the differences between underwater acoustics and terrestrial radio. These differences span physical propagation and energy consumption, and influence the design of medium access control, routing and topology management.

By first reviewing a simple model for underwater sound propagation and hardware energy consumption, we introduce a set of solutions which explicitly account for, or make use of, the longer propagation delays of acoustic waves in the water with respect to radio waves in the air, and the different ratio between transmit and receive energy consumption offered by underwater transducers. These protocols deal with the problems of efficiently scheduling transmissions in a fixed 3D deployment, of optimizing the use of energy by choosing the best mechanisms for topology management, and of choosing the best hop length over a multihop path.

We then review some more realistic underwater sound propagation behaviors, and detail their consequences on the simulation of MAC protocols for underwater networks. Finally, we briefly discuss the currently available underwater communications hardware (including both commercial and research modems) and comment on which paradigms are currently realizable, with special regard to those requiring the adaptability of transmit power and frequency.

Keywords: Underwater acoustic networks, Protocol design, Channel modeling

1. Introduction

Underwater acoustic networks are considered to be a future key asset in ocean monitoring, surveillance and patrolling missions, and have recently been attracting a lot of interest. The im-

Email addresses: casarip@dei.unipd.it (Paolo Casari), zorzi@dei.unipd.it (Michele Zorzi)

Preprint submitted to Computer Communications

June 14, 2011

portance of this new area of research, and the momentum underwater communications networks are gaining within the research community, are testified by the continued improvements and new proposals in the fields of signal processing, transceiver architectures and network protocol design, and have been discussed in several survey papers such as [1–5].

The application scenarios for underwater networks have gained increasingly wider scope, and range from simple telemetry (e.g., for pipeline surveillance or movement detection in littoral areas) to more complicated missions involving mobile submarines, that cooperate to track moving objects. Continued improvements in communication hardware and signal processing techniques (e.g., see [6]) have made underwater communications possible over the distances of interest for such applications. These distances range from a few hundred meters (domain of short-range, high-frequency acoustic modems) to one or more kilometers (for lower-frequency, long-range modems). Very recently, the design of underwater modems has been furthered by proposing reprogrammable hardware (e.g., [7, 8]), which gives the user at least some choices as to which communication protocol is being used, which data format, and so forth. In addition, some low-cost models [7] will allow a larger deployment size by reducing the price of network equipment.

This paper focuses on network protocols tailored for underwater acoustic networks. While inspired by solutions for wireless radio networks, these protocols must be adapted or even re-designed in order to match the underwater environment. In fact, acoustic communications underwater are characterized by three major differences with respect to terrestrial radio: the very low propagation speed [9]; the strongly anisotropic nature, whereby horizontal channels are usually harsher than vertical channels [10]; the significant difference between the power required to operate acoustic transducers and the power required to receive or listen to an acoustic signal [11].

Starting from a discussion on related work and from general considerations and simple models for underwater acoustic propagation, we will consider some protocol design solutions addressing specific underwater networking issues, and illustrate them by using some examples taken from our own recent work. In particular, we will discuss the impact of the underwater channel on access protocols for acoustic networks, and describe two approaches to scheduled access which are specifically tailored to underwater propagation [11, 12]. We will also show how the bandwidth-distance relationship found in underwater channels can be exploited to optimize the distance be-

tween subsequent relays over a multihop path [13]. Finally, we will discuss actual underwater sound propagation effects, and how they can be modeled to be included into a network simulator [14]. We will exemplify the impact of a more accurate channel model on the simulation of channel access protocols, and will conclude our paper with a review of current acoustic transmission technologies. The latter discussion is helpful to clarify which of the approaches described in this paper are actually achievable to date, which are not, and which will likely be in the near future.

2. Related work

2.1. Medium Access Control

We start by reviewing the main approaches to protocol design for underwater acoustic networks. Like in terrestrial radio networks, the basic problem of channel access was the first to be taken into account. A general discussion on **deterministic schemes**, based on Time-, Frequency- or Code-Division Multiple Access (TDMA, FDMA, CDMA) can be found in [1]. While deterministic access is a simple paradigm, its direct adoption in underwater networks is not necessarily a good solution. For example, due to acoustic modem limitations, **FDMA** was preferred for an initial deployment of SeaWeb [3, 15], one of the first underwater networks experimented at sea. However, FDMA is inherently inefficient, due to the need to allocate guard bands in order to keep signals separated [16], and to the lack of flexibility in bandwidth assignment. In turn, no user can be allowed a temporarily larger rate to accommodate, e.g., bursty traffic generation. A different approach to FDMA can be found in [17, 18], where sub-bands are allocated to transmitter-receiver links depending on the distance to be covered. The allocation is performed so that a link is operated on a frequency where the combined effect of attenuation and noise is low (see channel model in Section 3) and the network is optimized for max-min fairness. A similar approach is found in [19], where the authors optimize the assignment of subcarriers within an **Orthogonal FDMA** Medium Access Control (MAC) framework, with the objective of minimizing the overall energy consumption.

The main issue behind **TDMA** is instead its need for network synchronization [1]. Nevertheless, in some cases TDMA can offer an interesting option for contention-free communications. For

example, if a network is organized in clusters, and within a cluster all transmissions are between the children nodes and the cluster head, the usage of TDMA may in fact be advantageous [20–22]. In particular, the lack of need for further signaling messages allows to increase the transmission efficiency, once the TDMA schedule has been established [23, 24]. A more complex implementation of TDMA, which instead includes the periodic exchange of signaling messages in order to locally synchronize the awake/asleep schedules of the nodes, is proposed in [25].

CDMA has also been considered for underwater communications, in both its Frequency Hopping (FH) and Direct-Sequence Spread Spectrum (DSSS) versions. Like in radio, CDMA allows to differentiate between signals superimposed in both time and frequency, thereby requiring no coordination or synchronization among terminals. In addition, it is robust against frequency-selective channels and narrowband jammers, but requires to control the transmission power at all terminals, in order to counter the near-far problem. A further inconvenience comes from the need to support many users. DSSS achieves a good capability to cancel interfering signals when the ratio among the rate of the spreading sequence and the bit rate is sufficiently high (e.g., no less than 16), which leads to a low bandwidth available for data. In any event, a properly designed FH system has good multiple access efficiency and is robust to multipath, but requires in general a number of subbands that increases with the number of users. This translates into a lower data rate per user for a fixed total system bandwidth. Moreover, FH has been shown to lead to higher bit error rates than DSSS [26]. In [27], DSSS is paired up with multicarrier communications to achieve higher spectral efficiency, at the price of higher complexity. Single-carrier DSSS CDMA with power control using a mechanism inherited from radio is discussed in [28]. However, the resulting protocol may be not suitable for densely deployed nodes [29]. CDMA and TDMA have been jointly employed in the design of protocols for acoustic networks in [21, 30, 31].

Most of the efforts on underwater MAC have however focused on the design and performance evaluation of **random access protocols**, which have the advantage not to require synchronization, and to exploit the full bandwidth of the system. However, lack of coordination may lead to frequent interference from colliding transmissions, and hence to loss of data. This is the main problem of **ALOHA** in the presence of high traffic. **Slotted ALOHA**, where nodes share the same time synchronization and transmit only at the beginning of a time slot, has also been considered for

underwater communications. In this case, however, the efficiency is lower than in radio, due to the long guard times required to compensate for the different propagation delays in the network. In fact, in the presence of very high delays, slotted ALOHA may exhibit the same channel utilization as unslotted ALOHA [32]. In [33] the authors propose a variation of the protocol that reduces guard times and achieves benefits in the presence of a low ratio between the propagation delay and the data packet duration. A different approach [34] endows ALOHA with some memory of overheard transmissions, in order to decrease the likelihood of a collision.

Carrier-Sense Multiple Access (CSMA) has also been investigated. However, its performance is limited by the need that the packet transmission time should be much greater than the propagation delay, a condition that is rarely met in typical underwater networks, where the use of CSMA may lead to an exceedingly long vulnerability time. A simple form of CSMA, whereby the channel is listened to for a very short time, in order to avoid some transmission patterns surely resulting in collisions, has been proposed in [14] (see also the description of CSMA-ALOHA in Section 5.3) and shown to perform well, in spite of a possibly over-conservative behavior [34]. **CSMA with collision avoidance (CSMA-CA)** is also an option, which reduces the chance of collisions at the price of higher delays for connection establishment, due to the need to wait for the completion of the Request-To-Send/Clear-To-Send (RTS/CTS) exchange. The underwater emanation of **MACA** with packet trains proposed in [35, 36], **DACAP** [37] and **APCAP** [38] are good examples of the CSMA-CA mechanism. It has been shown that in certain cases the interference mitigation effect of the RTS/CTS exchange is beneficial [14]. Nevertheless, multihop topologies may be subject to additional problems, mainly caused by collisions among signaling and data packets. Packet fragmentation is proposed in [39] to counter this fact, whereas [40] makes use of a separate control channel for the RTS/CTS exchange, and [41] further extends this idea to multi-channel data communications. **Slotted FAMA** [42] adds a further requirement that the nodes be slot-synchronized, and that they transmit any packet (including RTSs and CTSs) only at the beginning of a slot. The resulting protocol experiences fewer collisions, but is also subject to longer delays imposed by guard times within slots. By removing the interaction with receivers, and by letting transmitters contend for channel access using tones, **Tone-Lohi** [43] tries to make the access process smoother yet distributed, at the price of greater vulnerability to the hidden terminal

effect.

Hybrid solutions switching between different schemes on demand or in a traffic-adaptive fashion have also been proposed. In [41] the protocol employs ALOHA until the traffic becomes too intense, after which it shifts to a MACA-like scheme. Similarly, **D-MAC** [44] prescribes that ALOHA be used for the transmission of short messages, whereas bulk data transmissions, with several packets sent back-to-back, are preceded by an RTS/CTS handshake. The protocol proposed in [45], instead, divides time in frames and advocates the switch from a contention-based (non-scheduled) to a contention-free (scheduled) protocol, which are configured as two separate phases of configurable duration within the same frame.

2.2. Routing

The problem of routing in underwater acoustic networks has received less attention compared to MAC. The approaches that have emerged are, in fact, mostly tailored around the characteristics of specific underwater communications scenarios. For example, in [46] the authors assume a typical topology made of a sea surface buoy acting as a sink, and gathering data from nodes underneath. The topology is detected via probes sent by the buoy, and returned upstream following the reverse of downstream routes. In [47], the authors focus on the delay performance, and propose two **routing algorithms for delay-sensitive and delay-insensitive applications** in a 3D underwater environment. The delay-sensitive algorithm is based on virtual circuit routing. Primary and backup multi-hop node-disjoint data paths are calculated by a centralized controller to achieve, e.g., optimal delay. The delay-insensitive algorithm is a distributed geographic solution aimed at minimizing the energy consumption via back-to-back packet transmissions and cumulative acknowledgments. **Vector-Based Forwarding (VBF)** [48, 49] is also a geographic approach, which prescribes that packets be forwarded without deviating too much from the route towards the final destination. Therefore, over a multihop path, only the nodes that are located within a pipe of given width between the source and the destination are considered for relaying. Similarly, **Focused-Beam Routing (FBR)** [50] prescribes that relays be picked among the nodes located within a cone whose vertex is the current transmitter. An RTS/CTS handshake is set up to isolate closer nodes within this cone, and farther nodes are sought only if no closer node is found. A

theoretical argument supporting geographic routing has been discussed in [13] based on simple propagation and energy consumption models for underwater networks. The study shows that an optimal number of hops along a path (according to, e.g., a minimum energy consumption criterion) exists, and that increasing the number of hops (by choosing closer relays) is preferable with respect to keeping the route shorter. In view of this, several position-based routing algorithms are proposed and compared; results show (see also Subsection 4.3) that selecting relays closer than a given maximum distance before seeking farther ones achieves in fact optimal energy consumption. The relay selection algorithm employed in FBR [50] also follows a similar approach.

Unlike the previous location-based solutions, **Depth-Based Routing (DBR)** [51] bases routing decisions on the nodes' depth, which is easily obtained via a pressure gauge. DBR is thus particularly suited for vertically deployed topologies, such as those considered in [46]. A similar idea can be found in [52], where relays are chosen based on a weighed average of advancement towards the sources and probability of packet delivery, and a recovery method is added to handle the absence of a relay node at lower depth than the current packet holder.

More specialized routing-related approaches such as **Phero-Trail** [53] have also been proposed for routing towards the latest known position of a mobile roaming through the network, and for **broadcasting** information over multihop topologies [54–56].

2.3. Transport and topology control

Only a few works deal with higher-level network functions such as **transport and topology control**. Among these, **SDRT** [57] proposes a segmentation and coding scheme based on erasure codes, to achieve better utilization of the underwater channel bandwidth; topology control is the focus of [58], which proposes a sparsification algorithm to select links that optimize power attenuation and transmission delay; a different view of topology control is proposed in [11], where the authors argue that **low-power listening** modes can be exploited easily in underwater networks to improve the effectiveness of channel access and link setup.

3. Simple models for underwater sound propagation and noise

The simplest model for underwater acoustic propagation considers the distance- and frequency-dependent attenuation of sound waves as the superposition of two main contributions: *i*) spreading, like in radio, whereby the wave front expands as it propagates, e.g., in a spherical pattern, distributing the initial energy over progressively wider surfaces; *ii*) absorption, which models the conversion of pressure into heat by the interaction of sound waves with salts suspended in water. (This second effect is negligible in radio.) The resulting model for the attenuation $A(d, f)$ affecting a tone of frequency f transmitted over a distance d has the form [9, 59]

$$10 \log_{10} A(d, f) = k \cdot \log_{10}(d_m) + d_{km} \cdot a(f), \quad (1)$$

where $a(f)$ is the absorption factor, which can be represented using (among others) Thorp's formula [9] and is measured in dB/km, d_m and d_{km} represent the distance traveled by the signal, expressed in meters and kilometers, respectively, d_0 is the reference distance, k is the spreading coefficient. Because $a(f)$ increases steeply with frequency, the use of high carrier frequencies is not convenient, even if the available bandwidth would be larger. By defining the Signal-to-Noise Ratio (SNR) of a tone transmitted at a certain frequency, it is actually possible to derive the optimal transmit frequency band and related -3 dB bandwidth for a given distance. Define the receive SNR of a tone at frequency f as the ratio of received power to noise in a narrow band around f , i.e.,

$$\text{SNR} = \frac{P_{\text{tx}} A(d, f)}{N(f) \Delta f}, \quad (2)$$

where P_{tx} is the transmit power, Δf is a narrow frequency window around f , and $N(f)$ is the power spectral density of the noise process, which can be empirically derived as in [9]. Noise is usually modeled as the result of a variety of causes, that include wind (as measured by the wind speed w) and shipping (indicating the amount of naval traffic near the network area, and expressed through a parameter $0 \leq S \leq 1$, where 0 corresponds to no shipping and 1 to a very busy shipping route). Higher values of either S or w turn into higher noise power, but this not the only effect. It is exactly the dependence on frequency of both $A(d, f)$ and $N(f)$ that causes the existence of an optimal transmit frequency f for a given distance d . Along the observations

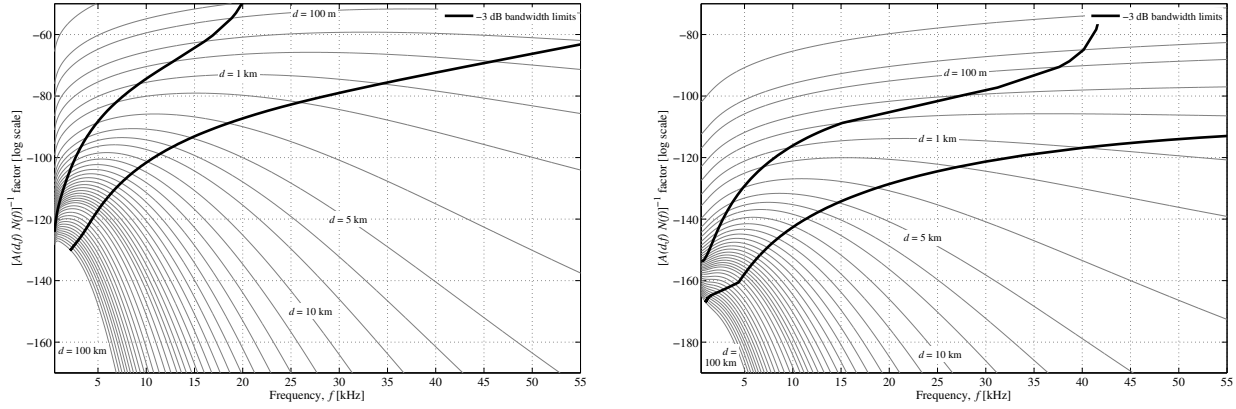


Figure 1: Frequency-dependent component of the SNR as a function of frequency f , for different distances d . Shipping factor $S = 0.5$, wind speed $w = 0$ m/s (left, from [54] © 2008 IEEE, reproduced with permission) and 30 m/s (right). Each grey line corresponds to a different distance. Thick solid black lines represent the lower and upper limits of the available bandwidth according to the empirical -3 dB definition.

in [59], let us consider the pictures in Figure 1, where the frequency-dependent factor of the SNR, $[A(d, f)N(f)]^{-1}$ (hereafter “AN factor” for short), is shown for various (fixed) distances, from a few tens of meters to tens of kilometers. Focus for the moment on the figure on the left, where we set $S = 0.5$ and $w = 0$. For each distance, the corresponding curve reaches a maximum at the optimal frequency to be used for a transmission at that distance, i.e., the frequency where the signal experiences the least combined effects of attenuation and noise. For each distance, the top and bottom limits of the -3 dB bandwidth have been computed as the frequencies where the AN factor is half its maximum value. The points have been joined to yield the two thick black curves delimiting the -3 dB bandwidth. These curves are also useful to observe that, as distance increases, the optimal frequency band for transmission moves toward the lower portion of the acoustic spectrum.

It is interesting to observe that in case of different shipping, the behavior stays the same, the only difference being the absolute value of $N(f)$, which increases for increasing S . Wind has instead a different impact, as it varies significantly the shape of $N(f)$, and correspondingly that of the AN factor [9, 59]. The effects of a wind of 30 m/s, at $S = 0.5$, can be observed in the picture on the right in Figure 1, where the different shape of $N(f)$ tends to flatten the fixed-distance

curves. While the noise power is certainly higher (requiring stronger transmit power to support communication at the same distance) the -3 dB bandwidth is actually a little larger, due to such flattening effect. System design can therefore be carried out by taking the values $S = 0.5$, $w = 0$ as a standard case, because the same frequencies would be supported as well in case of different shipping and stronger wind; however, it should be kept in mind that using the frequencies obtained for $w = 0$ in the presence of stronger wind is inefficient (the actual bandwidth of the system is in fact larger).

Albeit exceedingly simple and not very representative of actual underwater propagation (see Section 5.3), the above model already allows to develop some underwater channel-matched protocol design guidelines. For example, consider an FDMA system, where the N users have each $1/N$ th of the overall bandwidth available. In a sufficiently stable environment, where the frequency response of the channel and the distances among nodes do not change significantly in time, [17] proposes the max-min optimum solution for allocating frequency bands to users. In particular, the technique assigns lower-frequency bands to farther users, whereas high-frequency bands are reserved for closer users, which can employ them more profitably.

Propagation is not the only feature distinguishing underwater acoustics from terrestrial radio. Table 1 summarizes the main differences which have an impact on networking. In particular we highlight five of them: *i*) limited, distance-dependent bandwidth; *ii*) long propagation delays, typically on the order of hundreds of milliseconds; *iii*) high transmit energy consumption compared to any other transceiver state; *iv*) currently difficult experimentation for networks of significant sizes deployed in realistic environments; *v*) lack of comprehensive channel models, and no clear understanding of how a model can be simplified to be included in network simulators and yet yield meaningful or realistic results.

4. Aspects of network design and operation based on the simple propagation model

In the three following subsections, we will describe two different protocol solutions taken from the literature which target some of these issues: based on the above model for underwater propagation, and assuming that the same band must be shared among all network nodes, the first approach deploys an optimization framework for deployment, routing transmit power and scheduling in a

Underwater acoustics	Terrestrial radio
Low bandwidth (kHz)	High bandwidth (MHz)
Long prop delays (s)	Short prop delays (μ s)
Distance- <i>dependent</i> bandwidth	Distance-independent bandwidth
Frequency-dependent noise	Typically white noise
Energy costs: TX > RX > Idle \gg Sleep	Energy costs: TX \sim RX \sim Idle \gg Sleep
Bulky and expensive nodes	Small and cheap nodes
Lots known on PHY, networking still in its infancy	Lots of research done on all communications aspects
No comprehensive channel model yet	Accepted channel models
Few simulation tools available	Several simulation tools used
Hard to experiment	Easy to experiment

Table 1: Main differences between underwater acoustic networks and terrestrial radio networks.

3D underwater network [12]; the second argues that the much lower energy required by a node to listen than to transmit can be leveraged on in order to access the channel effectively [11].

4.1. *Optimal node placement, routing and scheduling in a converge-casting underwater 3D network [12]*

The network we consider here is a subsea environmental monitoring and relay network, which must route all data collected by the nodes to a common station, in this case a buoy placed on the surface. There are two main thrusts behind this approach: *i)* the propagation delays of acoustic waves underwater are sufficiently long that even transmissions starting at the same time from different nodes may reach the same receiver without overlapping in time; *ii)* proper setting of the transmit powers can lead transmissions at similar distances to actually cause little unintended interference, thereby allowing the receiver to capture the strongest packet even when superimposed to other transmissions. Basically, if the nodes are placed so that such propagation delay differences actually exist, one can solve the problem of jointly optimizing transmission scheduling, transmit power, as well as the way packets are routed towards the surface buoy, so that transmissions co-exist and delivery is completed with minimum total energy consumption.

The problem has been formulated as an integer linear programming problem in [12]. The solution comes in the form of a schedule of length T , which can accommodate an integer number

of packet transmissions, with the objective of minimizing the overall power consumption, and using the actual presence of a relay node at candidate positions and link activation sequences as the decision variables. The optimization is subject to the usual flow constraints in graphs, whereby the packets transmitted by all nodes at a given time should be no more than the sum of the generated and received packets until that time. In addition, all traffic should be delivered to the surface sink within T , and of course packets must be transmitted from (and relayed at) locations where a node actually exists. This first problem specification leads to the definition of a schedule. If this schedule presents no collisions, the problem is solved. Otherwise, physical interference constraints are added for the nodes experiencing concurrent packet receptions. These constraints prevent received packets from overlapping and causing harmful interference to each other; to modulate the receive time and avoid overlapping, one has to solve the problem again with the new constraints. The procedure continues this way until a collision-free schedule is found.

As an example, in Figure 2 [12] we exemplify a succession of link activations (the number in parentheses next to each arrow corresponds to the time slot in which the transmitter is active). The link schedule is determined taking into account the interference relationships in time and space of the different nodes involved. In particular, the schedule must avoid that (i) an interfering packet overlaps at the receiver with the intended packet, unless the power of the latter is sufficient to capture the receiver, and (ii) a node is scheduled to transmit and receive at the same time. Based on the relative distance of each pair of nodes, the times of arrival and received powers can be determined and used to establish an interference-free schedule. For example, in Figure 2(c), the links from node 15 to node 13 and from 13 to 18 can be operated simultaneously, as the time separation due to the propagation delay guarantees that node 13 can finish its own transmission before it starts receiving the packet transmitted by node 15.

4.2. Topology control via low-power wakeup modes [11]

One of the hot topics in wireless radio sensor networks is energy saving via awake/asleep duty cycles. By leveraging on network redundancy, one can let some nodes deactivate their radio and controller systems, effectively turning the node to sleep, thereby saving energy. Since duty cycles make the network topology very dynamic, one usually refers to duty cycling and management

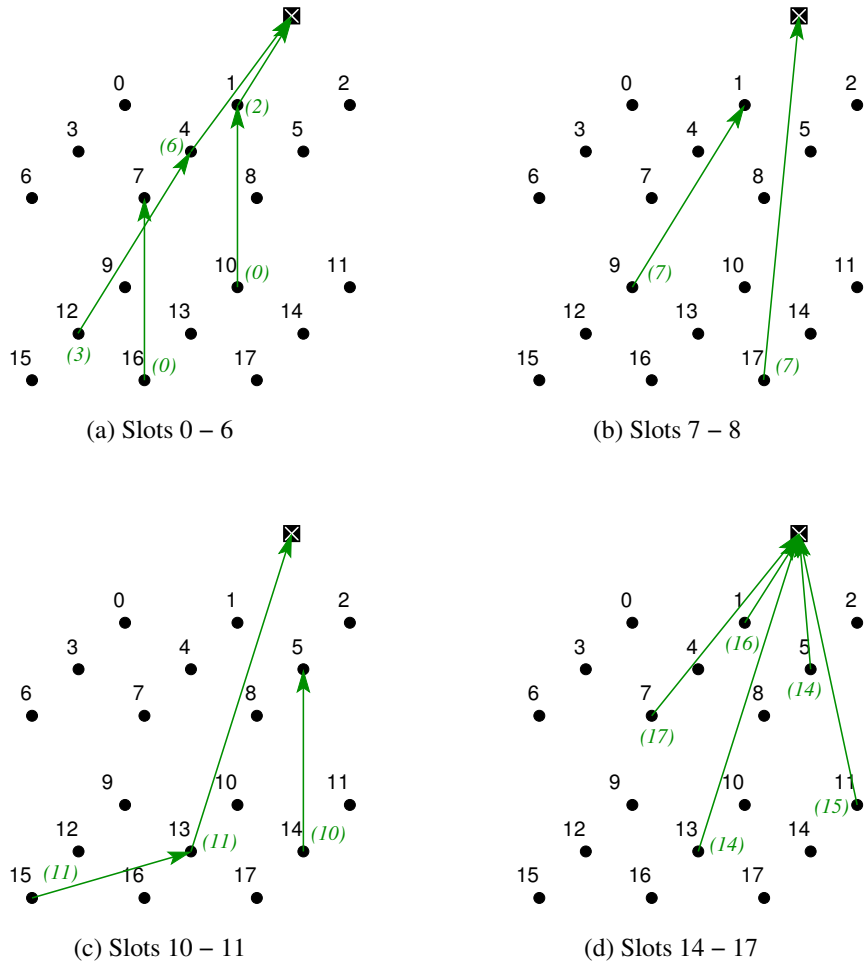


Figure 2: Example of schedule obtained via the integer programming framework presented in [12]. While the first phases (a) and (b) contain one transmission per slot, phase (c) as well as phase (d) allow concurrent transmissions, for those links that do not cause collisions. For example, two such links are $15 \rightarrow 13$ and $13 \rightarrow 18$ in (c), where time separation is enough for node 13 to transmit its own packet and receive a packet from 15 with no overlap [12].

thereof as topology control. In these schemes, two issues arise: on one hand, one should ensure that enough nodes are kept awake to maintain connectivity; on the other hand, a mechanism should exist to wake up nodes on demand, e.g., when a higher-level network protocol requires communication to a specific node, or when awake/asleep cycles are synchronized and all eligible forwarders of a node over a multihop path are asleep. For instance, STEM [60] is one solution to the second problem: it prescribes the transmission of wakeup signals which are short and frequent enough that at least one signal is received by any node in range during its awake period. When receiving

the wakeup signal, the node avoids going back to sleep and waits for a transmission to be set up.

Another way of realizing duty cycle management is via low-power wakeup hardware [61]. Such hardware keeps nodes in a listening mode where little energy is consumed, and is triggered by specific wakeup tones, long enough so that their energy can be detected. It has been observed that such kind of power management is necessary in radio in order to avoid the high consumption of an always-on system: radio transceivers and microcontrollers usually require similar power to transmit/receive a packet and to idly listen to the channel, while needing about two orders of magnitude less power in sleep mode.

However [11], the proportions are quite different for an underwater acoustic transceiver: the main power consumption takes place during transmission, whereas receive, idling and sleep phases are much less power-hungry. For instance, the WHOI micromodem hardware [62] can require up to 50 W for transmission, 2 W for reception and idle listening, 80 mW for wakeup and 40 mW for sleeping; similarly, the Teledyne-Benthos OEM modem [63] requires around 9 mW of wakeup power, whereas the SNUSE modem [64] requires around 0.5 mW. In addition, the use of low-power wakeup modes in underwater modems requires no additional receiver, unlike in radio nodes where a separate wakeup radio is needed. This observation is key to the use of continuous listening modes in underwater nodes, in place of awake/asleep cycles.

The results in [11] (see also Figure 3) compare the performance of four different approaches: a genie-aided optimal scheme, whereby nodes sleep maximally and know exactly when they should wake up; a scheme where node continuously receive; the STEM scheme; the wakeup scheme based on low-power idle listening. The figure on the left analyzes the performance at constant traffic as a function of the wakeup power, whereas the figure on the right varies traffic for constant wakeup power. The results in the first case show that STEM places itself between the optimum scheme and the always-listening scheme, whereas the wakeup mode can be more or less convenient than STEM, depending on the wakeup power. For power values aligned to those of the WHOI micromodem hardware [11, 62], Figure 3 on the right details the energy consumption as a function of traffic, showing that the wakeup scheme actually performs very close to the optimum, and is therefore very convenient to be implemented in underwater networks as a valid alternative to awake/asleep cycles.

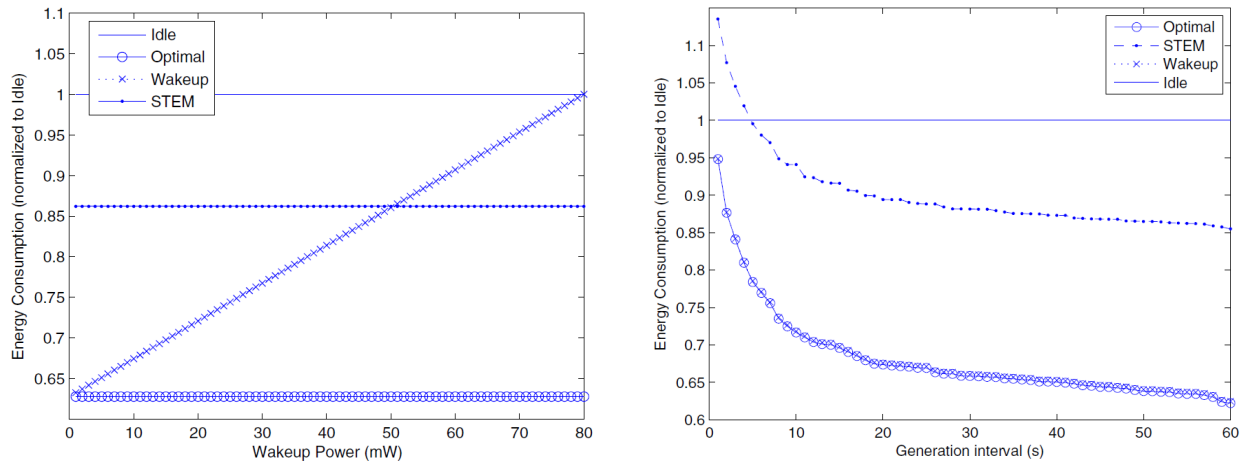


Figure 3: Comparison of the underwater low-power listening wakeup scheme against STEM [60], the always-on case, and a genie-aided optimal scheme: normalized energy consumption against the power consumption of the wakeup hardware for traffic generation rate of 1 packet per minute (left) and against the traffic generation interval for a wakeup power consumption of 1 mW (right). For reference, the WHOI micromodem requires a wakeup power of 80 mW, whereas Teledyne-Benthos off-the-shelf solutions require around 9 mW [63], and the SNUSE modem [64] around 0.5 mW. (From [11], © 2010 Elsevier.)

4.3. Optimal hop distance over a multihop path [13]

In many scenarios, the distances and the type of hardware employed will cause underwater networks not to be fully connected, so that a routing protocol is required. An interesting issue about routing is the following. Since the distance between two nodes, the power required to bridge the related link, and the bandwidth available to the link are strongly linked [59], is there an optimal distance at which a relay should be placed in order to, e.g., minimize the overall path energy consumption? In fact, long links not only require more transmit power, but also have a smaller bandwidth available (see Figure 1). In turn, this implies longer transmission times, hence higher energy spent for completing the transmission. Shorter links, instead, have the advantages of both a larger bandwidth and a lower power requirement, but a route of shorter links involves more relays, each incurring fixed energy costs for the reception of the signal from the relay upstream. However, given the strong convenience of shorter links, one may expect that their advantages mostly overcome the drawbacks. The balance between long and short links can be found by computing the power consumption per hop, given that a hop is at a certain distance. In particular,

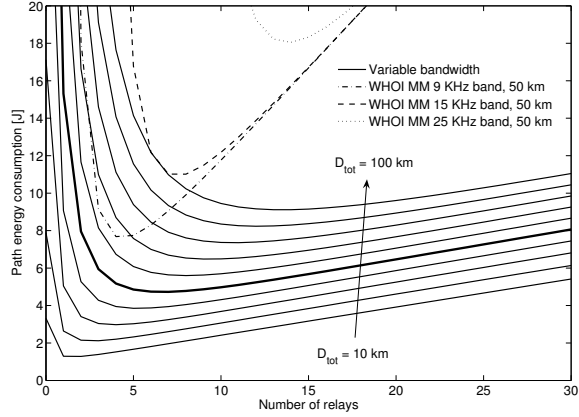


Figure 4: Energy consumption in a linear network as a function of the number of relays for different overall path length D_{tot} , under the assumption of perfect power and bandwidth control. For comparison, the fixed-bandwidth case of the WHOI micromodem (MM) bands is shown for a path distance of 50 km. (From [13] © 2008 IEEE. Reproduced with permission.)

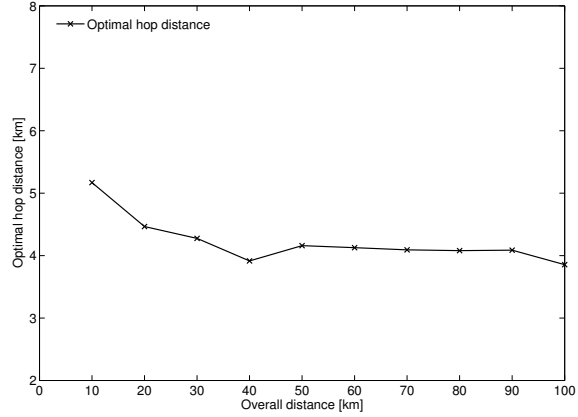


Figure 5: Optimal hop length in a 3D network as a function of the overall path distance. (From [13] © 2008 IEEE. Reproduced with permission.)

one can find [13]

$$\Delta_{\text{hop}}(\ell) = \frac{L}{\alpha B(\ell)} + \frac{\ell}{c}, \quad E_{\text{hop}}(\ell) = \frac{(P_r + P_t^{\text{el}}(\ell))L}{\alpha B(\ell)} \quad (3)$$

where $\Delta_{\text{hop}}(\ell)$ is the hop delay over a distance ℓ and is computed based on the length of the link L , the spectral efficiency of the modulation used α , the available bandwidth at a distance ℓ , $B(\ell)$, and the average propagation speed of sound, c . Similarly, $E_{\text{hop}}(\ell)$ is the energy consumption required to make the hop, computed as a function of the above quantities, as well as the receive power P_r , and the overall power consumed in transmit mode by the device, to generate a sound field able to cover a distance ℓ , i.e., $P_t^{\text{el}}(\ell)$. Approximate log-linear formulas [13, 59] can be used for $B(\ell)$ and $P_t^{\text{el}}(\ell)$.

The results of the computations as per the equations above are shown in Figure 4 [13], where we draw the variation of the overall path energy consumption over a path of distance D_{tot} from 10 to 100 km, as a function of the number of relays in between. The network considered here is linear, and the relays are assumed to be equally spaced. With solid lines, we denote the case of perfect power and bandwidth control, meaning that a transmission over a hop of given distance is

performed using the optimal power to cover the distance, and to fit the signal within the optimal -3 dB bandwidth available over that link. These curves show a very mild increase to the right, as opposed to a steep increase to the left; a minimum (optimum) point is identified in between. Figure 4 clearly suggests that an optimal number of relays for any given path length actually exists; also, moving away from the optimum to the right (i.e., increasing the number of relays) causes only a small increase in the path energy consumption, whereas decreasing the number of relays implies a much worse sub-optimality. This is a consequence of the double disadvantage experienced by long links, namely a higher power required and a smaller bandwidth, leading to longer time before a transmission is completed, thus higher energy consumption. These two factors easily overcome the only advantage of long links, that is, the lower number of relays and the related receive energy costs. The Focused Beam Routing protocol [50], also discussed in Section 2, implements this concept in practice by searching for closer relays before more distant ones are sought. In Figure 4, the above analysis is repeated for fixed-bandwidth hardware, while still assuming perfect power control. As an example, three of the WHOI micromodem bands have been selected for the comparison, and their performance over a path length of 50 km has been shown using dashed, dot-dashed and dotted lines; these can be directly compared to the thicker solid line of the perfect power and bandwidth control case over a link of the same length. We observe that the same arguments presented for the latter case still apply to the former: however, increasing the number of relays now presents one less advantage, in that the bandwidth cannot be adapted to fit the optimal settings for a given hop length. Hence, WHOI micromodem curves increase more steeply to the right.

Figure 5 shows the optimal hop length in a 3D network. Unlike in Figure 4, therefore, here we let the network be deployed randomly over a 3D volume, and find the average optimal hop distance as a function of the separation between the source and the destination. Even though the placement of the nodes in between is random, the results suggest that there is some kind of optimum hop length which holds constant almost regardless of distance. In order to pursue this optimum, let us consider the following position-based protocol (Bounded Distance from Below, BD-B, from now on): at each hop, find a node at distance equal to the optimal hop length D_{\max} (around 4 km as

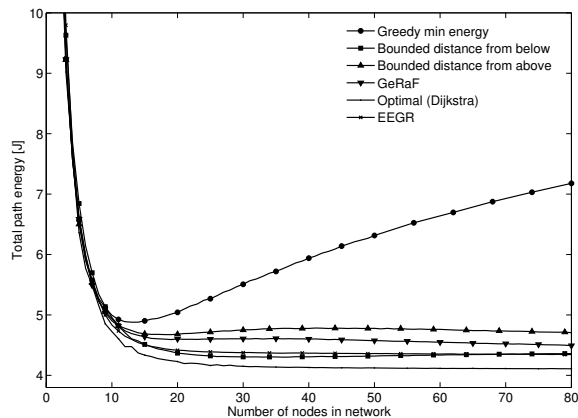


Figure 6: Energy consumption in a 3D network for different geographic relay selection strategies as a function of the number of nodes in the network. (From [13] © 2008 IEEE. Reproduced with permission.)

per Figure 5) in the direction of the receiver; if no such node is present, look for a closer node,¹ and if still unsuccessful try a farther node; as a last resort, transmit directly to the destination. In Figure 6, we compare this protocol to some competitors: *i*) its counterpart, Bounded Distance from Above (BD-A), whereby a node is sought at the optimal distance, then at a progressively farther distance, without looking for nodes within D_{\max} ; *ii*) GeRaF [65], whereby the farthest node within a distance of D_{\max} is always preferred; *iii*) Energy-Efficient Geographic Routing (EEGR), which seeks a relay to within a certain range of the intersection between the circle of radius D_{\max} centered at the current relay and the line joining the transmitter and receiver, and increases the search range until a relay is found; *iv*) an optimal genie-aided protocol, always choosing the least-energy route computed through a centralized algorithm; *v*) a greedy minimum energy protocol always choosing the least-energy hop, hence the closest relay. Figure 6 details the comparison for a total path length of 50 km, showing that the BD-B protocol and EEGR are very close to the centralized optimum, whereas, e.g., the greedy minimum energy protocol may choose too many relays, especially in dense networks, and thus requires more energy. The shortest path algorithm, transmitting directly from the source to the destination, consumes too much energy and is left out of the picture in order to magnify the differences between close-to-optimum protocols. Simulations performed using

¹We recall from Figure 4 that increasing the number of relays over a path by looking for closer nodes at every hop is less suboptimal than shortening the path by traveling longer hops.

ns2-Miracle in [13] also show that the BD-B can achieve a better energy-throughput tradeoff than EEGR, in that the minimum-energy points are comparable, whereas the throughput corresponding to the minimum energy point is significantly higher for BD-B.

5. Use of more realistic models for underwater acoustic propagation

5.1. Model description

While in Section 4 we described simple underwater link budget equations (Urick’s model [9]) and gave some examples of network design efforts based on that characterization, in this section we will delve into more detailed models for the behavior of sound propagating underwater. We will then show how these differences impact the accuracy of underwater networking simulations.

We start by recalling that water is a non-homogeneous propagation medium. In particular, the speed of sound in water (or equivalently, the water’s refraction coefficient) has a clear dependence on depth in any waters deeper than a few meters. In fact, the sound speed depends on three environmental factors: salinity, temperature (changing with depth because of the reduced radiation from the sun and the effect of the outside air temperature) and pressure (increasing with depth). The empirical relationship between these features and the density of water (and hence sound speed) is highly non-linear, and is called the state equation of the ocean (the current standard formula is based on work by Millero, Chen et al., and can be found in [66, 67]). A reasonably simpler form with an error of 0.07 m/s for salinity between 25 and 40 ppt is due to MacKenzie [68], whereas a different equation correcting possible discrepancies in the Chen-Millero formula is due to Del Grosso [69, 70].

When the speed of sound is not constant, the sound waves bend toward the direction of lowest speed, i.e., of lowest refraction index. This phenomenon, commonly observed in any non-homogeneous medium and actually exploited in fiber optics, gives rise to complex propagation behaviors for underwater sound waves, and also makes the characteristics of propagation very dependent on the geography and on the time of the year and even of the day. As an example, consider the pictures in Figure 7, which depict propagation at a currently typical carrier frequency of 25 kHz, in Tyrrhenian waters, respectively in summer and winter. The two figures have been ob-

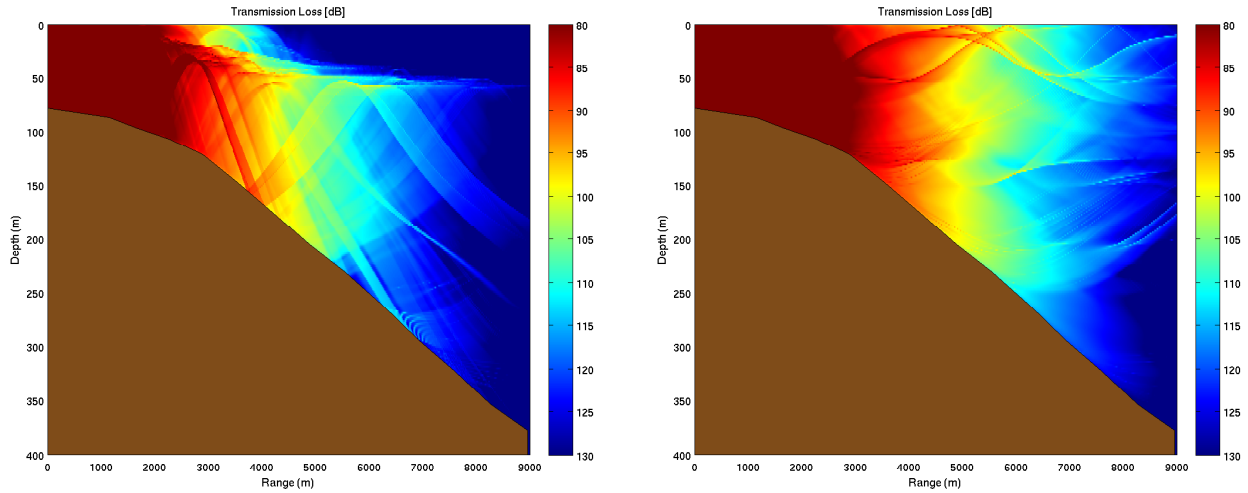


Figure 7: Profile of sound attenuation, expressed in dB, in the Tyrrhenian sea close to the Pianosa island in summer (left) and winter (right). Red hues correspond to a stronger signal. The frequency of the transmitted signal is 25 kHz.

tained via the Bellhop [71] tool for solving the propagation equation via a ray model [72, Chap. 3].² In summer, we observe a typically downward-refractive behavior: warmer waters at shallow depths cause the speed of sound to be higher than at lower depths. However, the limited depth at this site implies limited hydrostatic pressure, hence the sound speed close to the sea bottom does not increase at levels comparable to those at the surface. The result is that the sound wave front will always be bent downward, regardless of the number of bounces off the surface, bottom or both. For example, bottom bouncing waves will then be propagated forward and down again, and eventually experience more bounces before they reach the receiver. Due to downward wave bending, there may be portions of the water column which are notinsonified to an appreciable level. For example, this is the case in the top-right corner in the left picture of Figure 7.

The opposite situation is found in winter (Figure 7 on the right). Colder surface waters cause slower sound propagation, whereas the increase of pressure deeper down does the opposite. The

²In particular, the Gaussian beam shape and “incoherent” ray superposition options have been selected in the Bellhop configuration file. This means that the power of rays incident on any point is summed to yield the overall power at that point. Given the relatively limited channel delay spreads observed in this case, this operation is in accordance with the maximal-ratio combining capabilities of a good equalizer; in other words, signal processing at the receiver can extract energy from all received signal replicas.

resulting profile is typically upward-refractive, meaning that waves will be bent upward as they propagate, making surface bounces much more likely than bottom bounces. The pictures in Figure 7 show the overall effects of propagation in terms of the sound field attenuation, rather than the actual path of the sound waves; however, the downward- and upward-refractive behaviors are clearly observable in the shape of the portions of water where lowest attenuation takes place.

In deeper waters, these phenomena may give rise to more complex effects. For example, deep ocean waters with warm upper layers may cause the generation of a so-called deep sound axis channel, whereby most of the sound wave energy stays confined at a certain depth (around the minimum of the SSP), due to the downward refraction from the upper layers and upward refraction from the bottom layers [72, Ch. 1]. Similarly, in deep water upward refraction may lead to convergence zones, whereby signal replicas focus on the surface at points located at specific distances from the source, whereas nothing is heard between these points. It should be noted that in many of the scenarios above, some locations receive substantial insonification, as opposed to other portions which receive less or none at all. The latter are usually called shadow zones, in order to highlight the fact that sound is refracted away from these zones.

While Urick's propagation model [9] is enough for a first-order approximation to the performance of networks, when it comes to the simulation of specific scenarios with given morphology and environmental characteristics, actual propagation patterns should be implemented in a simulator. The next section explains how this has been accomplished in the World Ocean Simulation System (WOSS) [14, 73].

5.2. *Simulating networks with realistic sound propagation: the World Ocean Simulation System (WOSS)*

WOSS is a set of tools and primitives providing an almost seamless interconnection between Bellhop [71], the ray model-based simulator of acoustic propagation introduced before, and the popular network simulator ns2-Miracle [74]. In a nutshell, ns2-Miracle requires a measure of signal attenuation to be plugged in for the computation of Signal-to-Interference and Noise Ratios: instead of taking this measure directly from Urick's empirical equations, we run one or more Bellhop instances to obtain a more accurate attenuation value. Bellhop requires a full description of

the environment in order to compute sound propagation, and part of this description depends on data available to the network simulator, e.g., the current position of the nodes. WOSS is the key to realize the interaction between the two components. From ns2-Miracle, WOSS reads the geographic position of the nodes taking part in the communication, which includes the transmitter and receiver, as well as all neighboring nodes potentially reached by significant interference. WOSS then queries oceanographic databases to gather the specifications of the environment, given the geographic location of the nodes. Finally, it filters this information, e.g., by taking seasonal or monthly averages of the SSP, by adding random perturbations to the SSP and surface profiles, or by filling in unknown data via interpolation from known data. These operations result in a Bellhop configuration file, which is employed to run the ray tracing and retrieve the power-delay profile of the channel between a transmitter and its receivers (both wanted and unintended). From the power-delay profile, attenuation is derived by taking into account the capabilities of the receiver (repeating the example above, a receiver with an ideal equalizer may be modeled by computing the attenuation over the link as the L_2 -norm of the channel).

The type of information Bellhop requires is diverse, and fortunately mostly retrievable from free ocean databases. Specifically, SSPs are taken from the World Ocean Atlas [75], the profile of the bottom is provided by the GEneral Bathymetric Chart of the Oceans (GEBCO) [76], while the type of bottom sediments is derived from the DECK41 database [77]. The parameters that model the interaction between sound waves and the sea bottom have been taken from the literature (e.g., see [78–83]) given the type of bottom sediments provided by DECK41.

Other than standard features such as coordinate conversion and fly-of-bird trajectory computation for long-haul, constant-depth movements, WOSS also provides more advanced features. The available routines allow easy data manipulation (e.g., to add random offsets); this is useful to prepare a number of randomized realizations of the same channel, and can be employed, e.g., to implement channel variation in time. In addition, one can extend WOSS's interfaces toward oceanic databases in order to include any other environmental data in the simulations. One can also activate the inclusion of realistic transducer beam patterns in the computation of acoustic propagation (also a feature supported by Bellhop). WOSS comes with a set of toroidal and conical beam patterns taken from commercial hardware, which can be arbitrarily oriented in the up-down

left-right direction; the package will then automatically compute the projection of the beam pattern over the vertical slice of water where Bellhop computes sound propagation.

5.3. Comparison of network simulation results using Urick's equations and WOSS [14]

In the following, we present how protocol performance results may differ when modeling the channel via ray models through the Bellhop tool and the WOSS interface, as opposed to employing Urick's empirical equations; we note that the latter case corresponds to computing the propagation of a single ray under a constant sound speed assumption: therefore, attenuation is completely deterministic, and depends only on frequency and on the line-of-sight distance between the transmitter and the receiver.

For our comparison, we will consider three different protocols: a version of CSMA-ALOHA featuring a short clear channel assessment of random duration [14]; the "aggressive" version of the Tone-LOHI protocol [43]; the Distance-Aware Collision Avoidance Protocol (DACAP) [37]. Each protocol prescribes a different level of handshaking for the coordination of channel access procedures. In particular, CSMA-ALOHA presents no coordination, except for a short channel sensing phase to avoid starting a transmission while another acoustic signal is already propagating towards the receiver; Tone-Lohi is a transmitter-driven contention-based protocol which does not require heavy signaling burden in the presence of low traffic, but is prone to the hidden terminal problem, because receivers take no part in preliminary signaling; finally, DACAP is a full-fledged 3-way handshaking protocol (4-way in case ACKnowledgement packets are employed to detect transmission errors), with further refinements to avoid some collision events. Our study also aims at comparing the effectiveness of these approaches. We will now review briefly the functionalities of the protocols.

CSMA-ALOHA is an ALOHA enhancement. It prescribes that nodes sense the channel for a short, random-length time, in order to avoid a trivial collision event: assume that nodes A, B and C are roughly aligned, and A transmits to C. If B has a transmission for any other node, and starts the transmission while the signal from A is propagating over B, the two signals would very likely collide at C. The short channel sensing provides a means to avoid this situation. In case the channel is sensed busy, the node keeps listening until the transmission is completed, as this does

not consume too much power [11]. Immediately thereafter, a further channel sensing phase (again of random length) is scheduled, and the process goes on until the channel is finally sensed clear, after which the transmission is issued. CSMA-ALOHA can be operated with ACKs as well: in this case, a random exponential backoff is added in case of a wrong packet transmission or in case the ACK packet is lost.

Tone-Lohi [43] is based on the following mechanism. Before transmission, a sender issues a short busy tone (which can be used as well as a wakeup tone, if the hardware supports wakeup modes); this tone also serves as a warning to nearby contending transmitters. After the tone, the sender waits for a certain time, and if it hears no tone from any other node, the transmission starts immediately; otherwise, it counts the number of received tones and chooses a random backoff period which depends on the number of tones heard (the greater the number, the longer the average backoff period). If another tone is heard during the backoff period, the node exits the contention. Otherwise, it will send another tone at the end of the backoff, and the whole procedure restarts (possibly with a lower number of contenders); ultimately, there will be only one node sending a tone, and therefore transmitting the data packet. By tuning the length of the listening time after the tone transmission, a more aggressive or more conservative behavior can be set: the longer the time, the more conservative the protocol. Tone-Lohi can also include the transmission of ACKs after correct packet reception: as in ALOHA, an exponential backoff state is entered in case an ACK is not received.

DACAP is based on the exchange of Request-To-Send (RTS) and Clear-To-Send (CTS) packets to avoid interference from within a certain distance from the transmitter and the receiver. In addition, packet transmissions are deferred to allow overhearing of nearby signaling traffic, thereby detecting the chance of collisions in advance. In case potentially interfering traffic is taking place in the proximity of the receiver, there is an option to warn the transmitter through a specific packet. The length of the defer time is tunable: by prolonging it, collisions with signals from progressively lower-power interferers are avoided. DACAP can be configured to work with or without ACK packets: in the former case, timers have to be modified with respect to the latter.

The no-ACK versions of the three protocols described above have been simulated using Urick's model and the results have been compared to those obtained using ray tracing via Bellhop and the

WOSS interface. The network topology and the settings of the simulation can be found in [14], and are summarized here for convenience. The geographic location of the network is set to be East of the Pianosa island, off the Tyrrhenian coast of Italy, where many sea trials have been performed by the NATO Undersea Research Centre of La Spezia, Italy. From a morphological point of view, this implies a bathymetric profile of mildly increasing depth, warm waters, maximum depths on the order of 200-400 m, and sandy-muddy bottom sediments. (We recall that such environmental settings as required to run Bellhop, whereas they do not matter for the Urick case.)

The network is made of 10 nodes, placed on a 5×2 grid, with nearest neighbors 1 km apart. A sink buoy is placed on the surface at the center of the network deployment. The transceiver communicates with a bit rate of 4800 bps, akin to one of the WHOI micromodem's modes of operation. The packet size is 600 Bytes. Traffic is generated according to a Poisson process of average value λ bits per second per node. All traffic is directed toward the sink, which in turn is within direct coverage of all nodes. We note, however, that the network is not completely connected, as nodes at opposite sides of the grid (e.g., the 1st and the 5th on the longest side) would not receive a sufficiently powerful signal from each other, as computed using Urick's equations. Figure 8 reports the overall throughput of the network normalized to the channel capacity (here, equal to the maximum bit rate allowed by the modulation used, i.e., 4800 bps). The results of the simulation with Bellhop and WOSS are shown with gray curves, whereas black curves represent the case of Urick's equations. The first thing we note is that Urick simulations predict higher throughput than WOSS simulations. In fact, it has been observed [14] that the attenuation of the signal obtained through WOSS is higher than with Urick. This causes more frequent packet errors and therefore lower throughput. However, the difference between WOSS and Urick is not limited to a simple scale factor, as the ranking of the protocols also changes. Specifically, with Urick, ALOHA is first, aT-Lohi second and DACAP third. With WOSS, DACAP becomes second in rank. The reason of this change is, again, the increased attenuation predicted by WOSS, which in turn amplifies the hidden terminal effect to which aT-Lohi is prone. Namely, far nodes transmitting to the sink will be unlikely to hear nodes on the opposite side of the network. This will make them detect no contending transmitter, increasing the chance of collision, especially at high traffic. Albeit simple, this use case exemplifies the importance of detailed channel models when simulating the performance

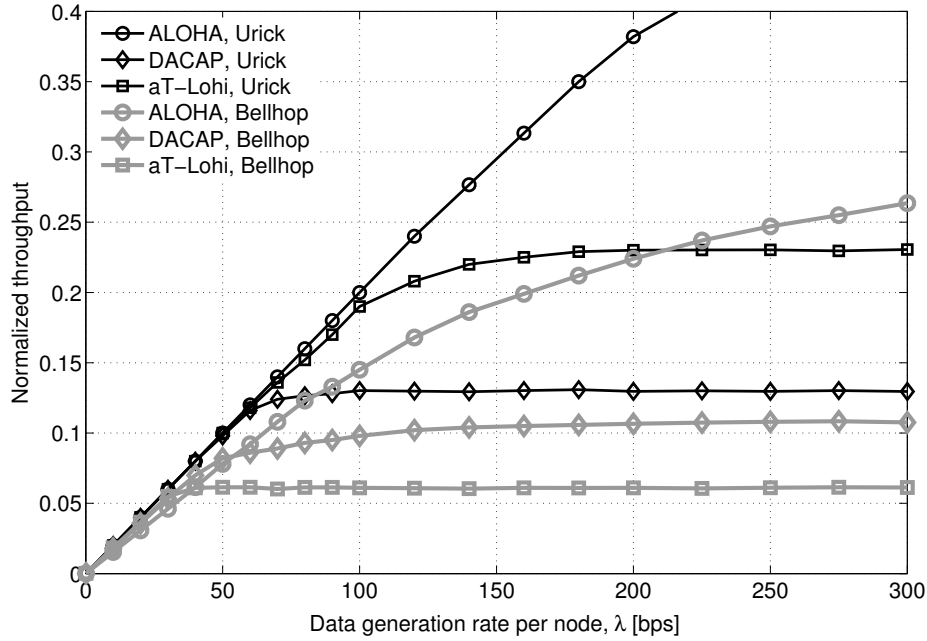


Figure 8: Comparison of normalized throughput achieved by the CSMA-ALOHA, Tone-Lohi and DACAP protocols in a network of 10 nodes with a common sink. Results are obtained both using Urick’s equations (black lines) and using WOSS (grey lines).

of the network in a specific scenario.

As a final note, ray tracing via Bellhop is a very computationally intensive effort, and requires to make some simplifying assumptions about channel variability in order to keep simulation times reasonable. For example, in static network topologies like the one considered above, one can assume quasi-static channel realizations, and possibly re-calculate the attenuation at regular intervals, adding each time a different random displacement to the SSP. This would simulate environmental variations and their impact on the acoustic channel. In dynamic topologies, such as the fully mobile network described in [84], the number of Bellhop runs to be performed increases considerably. In particular, if one re-computes the attenuations every time the nodes move, simulations could last up to several weeks. To decrease complexity, one has to resort to approximations. For example, instead of associating attenuation to pairs of nodes, one can associate attenuation to pairs of locations in the network area, one for the transmitter and one for the receiver; attenuation can then be assumed to be the same if the transmitter and receiver of a subsequent signal

are located within a given range of the original positions for which the attenuation was computed. Furthermore, if signals traveling across long acoustic links can be assumed to be heavily attenuated and therefore can be ignored, the ray tracing computational effort can be reduced, thereby shortening the simulation time. Nevertheless, the accuracy of either approach depends on the geographic location of the network and on the characteristics of the environment, and should thus be evaluated on a per-case basis.

6. On the capabilities of currently available hardware and modems

In this section, we discuss the capabilities of current modem hardware implementations and comment on their degree of reconfigurability. We start by recalling that from a networking point of view, there are three meaningful ways to change the configuration of an acoustic transceiver: the first regards protocol operations, packet formatting, timings and general management of communication activities; the second entails more physical layer-related processing, such as channel coding schemes; the third involves the whole physical layer via the reconfiguration of the modulation schemes and processing. These three categories have been ordered according to how deep the changes in the functionalities are.

To better grasp such issues, we should distinguish between commercial and research modems. Both are usually driven by controlling hardware (e.g., an embedded computer) via a serial connection. Recent work [15, 85] shows that substantial steps are being made towards the implementation of reconfigurable protocols using this simple structure. Now, changing a protocol usually requires spreading a different firmware through some reliable adaptive broadcasting method, which is a common operation in terrestrial radio sensor networks [86, 87]. However, most commercial modems do not currently support arbitrary firmware updates, not even if these changes are limited to, e.g., the way communications are administered, or the format of the output bitstream. Indeed, some exceptions exist: for example, the WHOI micromodem [62] and the Evologics S2C modems [88] support the transmission of short packets (minipackets in the micromodem jargon), which are completely customizable by the user, and transmitted subject to no particular MAC rule. Nevertheless, these packets are very short (on the order of tens of bytes) and do not leave much room for the implementation of complex protocols. However, for what concerns commercial

modems, using short messages as packets is the only way to implement one's own protocols on available hardware.

Research modems go one step beyond in this regard. Born to natively support development, frequent reconfigurations and changes, research modems usually embed FPGAs, DSPs and similar reprogrammable chips. Some designs even provide more complex structures including more high-level controllers such as embedded computers, instead of resorting to a single FPGA. The latter structure, in particular, does not have the firmware size limitations of an FPGA, and sacrifices some speed in favor of an even higher level of reconfigurability.

Table 2 presents some off-the-shelf and research acoustic modems (either already available or currently being developed). From the table, we see that many commercial designs have been advanced to a satisfactory performance level, in terms of supported bit rate, communications range, bit error rate and power consumption. Some architectures include storage space for data acquisition and later processing. Among the research modems [7, 8, 64, 89–93], some of which are still in active development, we highlight the well known WHOI micromodem, which is however available outside the US only in its least-capable form, i.e., the 80-bps non-coherent Binary FSK version, and the UC San Diego low-cost modem [7], whose hardware has been specifically chosen and designed to yield a low final price of a few hundred dollars. This modem can be reconfigured down to the format of transmitted packets, even though the modulation (which indeed yields acceptable performance for underwater networking tests) is fixed.

Other research modems are generally characterized by different levels of reconfigurability: some embed DSPs which allow to change the format of the transmitted signal, even though most fix the modulation scheme and receiver-side signal processing, while still permitting a full specification of the packet format. At this level, an end user may even decide to incorporate some form of channel (bit- or packet-level) coding, and hard or erasure decoding at the receiver. FPGA-based hardware is very suitable for this: one could implement coding and decoding on FPGAs, while still leaving the bulk of protocol operations to an external embedded PC, as serial connections are accepted by almost all modem designs.

7. Conclusions

To conclude our review of protocol design issues for the challenging scenario of an underwater acoustic network, we recall its three main differences with respect to terrestrial radio: distance-dependent bandwidth; different proportions of energy consumption in underwater modem states; different channel behavior and strong dependence of this behavior on the surrounding environment. These characteristics lead to changing the behavior of acoustic protocols in order to circumvent (or sometimes leverage on) these differences. Current research modem implementations allow some degree of reconfigurability, even though most commercial modems do not. However, it should be noted that all modems have fixed bandwidth occupancy due to transducer constraints, which in turn limits the applicability of bandwidth-adaptive protocols. However, current research on OFDM modems, along with the existence of some transducers with a flat response over a wide portion of the acoustic spectrum, encourages to think that these limits will be partly overcome in the future. Finally, a word should be spent on underwater acoustic propagation models suitable to be employed in underwater networking simulators. Currently, only three options are available: *i*) the employment of empirical attenuation equations; *ii*) embedding a propagation equations solver in a network simulator; *iii*) using channel traces recorded during sea trials. The first solution is useful for a first-order approximation of results, but not accurate for the simulation of a specific scenario and of specific environmental conditions; the second is more precise, but requires a large amount of computational effort, especially when simulating mobile networks; the third is very location- and time-dependent, as specific traces tend to be valid only when simulating the same conditions found when acquisition was performed. A compact, comprehensive channel model for use in simulation software is however still missing, and is definitely a worthwhile future research effort.

References

- [1] E. M. Sozer, M. Stojanovic, J. G. Proakis, Underwater acoustic networks, *IEEE J. Ocean. Eng.* 25 (1) (2000) 72–83.
- [2] J. Heidemann, W. Ye, J. Wills, A. Syed, Y. Li, Research challenges and applications for underwater sensor networking, in: *Proc. of IEEE WCMC, Las Vegas, NV, 2006.*

- [3] J. Partan, J. Kurose, B. Levine, A survey of practical issues in underwater networks, in: Proc. of ACM WUWNet, Los Angeles, CA, 2006.
- [4] I. F. Akyildiz, D. Pompili, T. Melodia, Underwater acoustic sensor networks: research challenges, Elsevier Ad Hoc Networks 3 (3) (2005) 257–279.
- [5] D. Pompili, I. Akyildiz, Overview of networking protocols for underwater wireless communications, IEEE Commun. Mag. 47 (1) (2009) 97–102.
- [6] M. Chitre, S. Shahabudeen, M. Stojanovic, Underwater acoustic communications and networking: Recent advances and future challenges, Marine Tech. Soc. Journal 42 (1) (2008) 103–116.
- [7] B. Benson, Y. Li, B. Faunce, K. Domond, D. Kimball, C. Schurgers, R. Kastner, Design of a low-cost underwater acoustic modem, IEEE Embedded Syst. Lett. 2 (3) (2010) 58–61.
- [8] S. Mason, R. Anstett, N. Anicette, S. Zhou, A broadband underwater acoustic modem implementation using coherent OFDM, in: Proc. of NCUR, Dominican University of California, CA, 2007.
- [9] R. Urick, Principles of Underwater Sound, McGraw-Hill, New York, 1983.
- [10] L. Freitag, S. Singh, Performance of Micro-Modem PSK signaling under variable conditions during the 2008 RACE and SPACE experiments, in: Proc. of MTS/IEEE Oceans, Biloxi, MS, 2009.
- [11] A. F. Harris III, M. Stojanovic, M. Zorzi, Idle-time energy savings through wake-up modes in underwater acoustic networks, Elsevier Ad Hoc Networks 7 (4) (2009) 770–777.
- [12] L. Badia *et al.*, An optimization framework for joint sensor deployment, link scheduling and routing in underwater sensor networks, in: Proc. of ACM WUWNet, Los Angeles, CA, 2006.
- [13] M. Zorzi, P. Casari, N. Baldo, A. F. Harris III, Energy-efficient routing schemes for underwater acoustic networks, IEEE J. Sel. Areas Commun. 26 (9) (2008) 1754–1766.
- [14] F. Guerra, P. Casari, M. Zorzi, World Ocean Simulation System (WOSS): a simulation tool for underwater networks with realistic propagation modeling, in: Proc. of ACM WUWNet, Berkeley, CA, 2009.
- [15] J. Rice, SeaWeb acoustic communication and navigation networks, in: Proc. of IACM UAM, Heraklion, Greece, 2005.
- [16] J. Gibson, A. Larraza, J. Rice, K. Smith, G. Xie, On the impacts and benefits of implementing full-duplex communications links in an underwater acoustic network, in: Proc. of 5th International Mine Symposium, Monterey, CA, 2002.
- [17] N. Baldo, P. Casari, M. Zorzi, Cognitive spectrum access for underwater acoustic communications, in: Proc. of IEEE ICC CogNet Workshop, Beijing, China, 2008.
- [18] N. Baldo, P. Casari, P. Casciaro, M. Zorzi, Effective heuristics for flexible spectrum access in underwater acoustic networks, in: Proc. of MTS/IEEE Oceans, Québec City, Canada, 2008.
- [19] M. Hayajneh, I. Khalil, Y. Gadallah, An OFDMA-based MAC protocol for under water acoustic wireless sensor networks, in: Proc. of IWCMC, Leipzig, Germany, 2009.

- [20] F. Salva-Garau, M. Stojanovic, Multi-cluster protocol for ad hoc mobile underwater acoustic networks, in: Proc. of MTS/IEEE Oceans, San Diego, CA, 2003.
- [21] P. Casari, S. Marella, M. Zorzi, A comparison of multiple access techniques in clustered underwater acoustic networks, in: Proc. of IEEE/OES Oceans, Aberdeen, Scotland, 2007.
- [22] M. Cardei, Energy-efficient scheduling and hybrid communication architecture for underwater littoral surveillance, Elsevier Computer Communications 29 (17) (2006) 3354–3365.
- [23] Y. Ma, Z. Guo, Y. Feng, M. Jiang, G. Feng, C-MAC: A TDMA-based MAC protocol for underwater acoustic sensor networks, in: Proc. of NSWCTC, Wuhan, China, 2009.
- [24] L. Hong, F. Hong, Z. Guo, X. Yang, A TDMA-based MAC protocol in underwater sensor networks, in: Proc. of WiCOM, Dalian, China, 2008.
- [25] M. K. Park, V. Rodoplu, UWAN-MAC: an energy-efficient MAC protocol for underwater acoustic wireless sensor networks, IEEE J. Ocean. Eng. 32 (2007) 710–720.
- [26] L. Freitag, M. Stojanovic, S. Singh, M. Johnson, Analysis of channel effects on direct-sequence and frequency-hopped spread-spectrum acoustic communication, IEEE J. Ocean. Eng. 26 (4) (2001) 586–593.
- [27] D. Kalofonos, M. Stojanovic, J. Proakis, Performance of adaptive MC-CDMA detectors in rapidly fading Rayleigh channels, IEEE Trans. Wireless Commun. 2 (2) (2003) 229–239.
- [28] D. Pompili, T. Melodia, I. Akyildiz, A CDMA-based medium access control for underwater acoustic sensor networks, IEEE Trans. Wireless Commun. 8 (4) (2009) 1899–1909.
- [29] G. Shah, A survey on medium access control in underwater acoustic sensor networks, in: Proc. of WAINA, Bradford, UK, 2009, pp. 1178–1183.
- [30] M. K. Watfa, S. Selman, H. Denkilkian, UW-MAC: an underwater sensor network MAC protocol, Wiley Journal of Communication Systems 23 (4) (2010) 485–506.
- [31] R. Diamant, L. Lampe, A hybrid spatial reuse MAC protocol for ad-hoc underwater acoustic communication networks, in: Proc. of IEEE ICC, Cape Town, South Africa, 2010.
- [32] L. F. M. Vieira, J. Kong, U. Lee, M. Gerla, Analysis of ALOHA protocols for underwater acoustic sensor networks, in: Proc. of ACM WUWNet, Los Angeles, CA, 2006.
- [33] A. A. Syed, W. Ye, J. Heidemann, B. Krishnamachari, Understanding spatio-temporal uncertainty in medium access with ALOHA protocols, in: Proc. of ACM WUWNet, Montréal, Canada, 2007.
- [34] N. Chirdchoo, W.-S. Soh, K. C. Chua, ALOHA-based MAC protocols with collision avoidance for underwater acoustic networks, in: Proc. of IEEE INFOCOM, Anchorage, AK, 2007.
- [35] N. Chirdchoo, W.-S. Soh, K. C. Chua, MACA-MN: A MACA-based MAC protocol for underwater acoustic networks with packet train for multiple neighbors, in: Proc. of IEEE VTC Spring, Singapore, 2008.
- [36] N. Chirdchoo, W.-S. Soh, K. Chua, RIPT: A receiver-initiated reservation-based protocol for underwater acoustic networks, IEEE J. Sel. Areas Commun. 26 (9) (2008) 1744–1753.

- [37] B. Peleato, M. Stojanovic, Distance aware collision avoidance protocol for ad hoc underwater acoustic sensor networks, *IEEE Commun. Lett.* 11 (12) (2007) 1025–1027.
- [38] X. Guo, M. Frater, M. Ryan, Design of a propagation-delay-tolerant MAC protocol for underwater acoustic sensor networks, *IEEE J. Ocean. Eng.* 34 (2) (2009) 170–180.
- [39] S. Basagni, C. Petrioli, R. Petroccia, M. Stojanovic, Choosing the packet size in multi-hop underwater networks, in: *Proc. of IEEE Oceans*, Sydney, Australia, 2010.
- [40] L. T. Tracy, S. Roy, A reservation MAC protocol for ad-hoc underwater acoustic sensor networks, in: *Proc. of ACM WUWNet*, San Francisco, CA, 2008.
- [41] Z. Zhou, Z. Pengt, J.-H. Cui, Z. Jiang, Handling triple hidden terminal problems for multi-channel MAC in long-delay underwater sensor networks, in: *Proc. of IEEE INFOCOM*, San Diego, CA, 2010.
- [42] M. Molins, M. Stojanovic, Slotted FAMA: a MAC Protocol for underwater acoustic networks, in: *Proc. of MTS/IEEE Oceans*, Singapore, 2006.
- [43] A. Syed, W. Ye, J. Heidemann, Comparison and Evaluation of the T-Lohi MAC for Underwater Acoustic Sensor Networks, *IEEE J. Sel. Areas Commun.* 26 (2008) 1731–1743.
- [44] O. Kebkal, M. Komar, K. Kebkal, D-MAC: Hybrid media access control for underwater acoustic sensor networks, in: *Proc. of IEEE ICC*, Cape Town, South Africa, 2010.
- [45] K. B. Kredo II, P. Mohapatra, A hybrid medium access control protocol for underwater wireless networks, in: *Proc. of ACM WUWNet*, Montréal, Canada, 2007.
- [46] G. G. Xie, J. H. Gibson, A network layer protocol for UANs to address propagation delay induced performance limitations, in: *Proc. of MTS/IEEE Oceans*, Honolulu, HI, 2001.
- [47] D. Pompili, T. Melodia, I. F. Akyildiz, Routing algorithms for delay-insensitive and delay-sensitive applications in underwater sensor networks, in: *Proc. of ACM MOBICOM*, Los Angeles, CA, USA, 2006.
- [48] P. Xie, J.-H. Cui, L. Lao, VBF: Vector-based forwarding protocol for underwater sensor networks, in: *Networking 2006*, Vol. 3976 of *Lecture Notes in Computer Science*, Springer, 2006, pp. 1216–1221.
- [49] N. Nicolaou, A. See, J.-H. Cui, D. Maggiorini, Improving the robustness of location-based routing for underwater sensor networks, in: *Proc. of MTS/IEEE Oceans*, Vancouver, Canada, 2007.
- [50] J.-M. Jornet Montaña, M. Stojanovic, M. Zorzi, On joint frequency and power allocation in a cross-layer protocol for underwater acoustic networks, *IEEE J. Ocean. Eng.* 35 (4) (2010) 936–947.
- [51] H. Yan, Z. Shi, J.-H. Cui, DBR: Depth-based routing for underwater sensor networks, in: *Proc. of IFIP Networking*, Singapore, 2008.
- [52] U. Lee, P. Wang, Y. Noh, F. M. L. Vieira, M. Gerla, J.-H. Cui, Pressure routing for underwater sensor networks, in: *Proc. of IEEE INFOCOM*, San Diego, CA, 2010.
- [53] F. M. L. Vieira, U. Lee, M. Gerla, Phero-trail: a bio-inspired location service for mobile underwater sensor networks, in: *Proc. of ACM WUWNet*, San Francisco, CA, 2008.

- [54] P. Casari, M. Rossi, M. Zorzi, Towards Optimal Broadcasting Policies for HARQ based on Fountain Codes in Underwater Networks, in: Proc. of IEEE/IFIP WONS, Garmisch-Partenkirchen, Germany, 2008.
- [55] P. Casari and A. F. Harris III, Energy-efficient reliable broadcast in underwater acoustic networks, in: Proc. of ACM WUWNet, Montréal, Canada, 2007.
- [56] P. Nicopolitidis, G. Papadimitriou, A. Pomportsis, Adaptive data broadcasting in underwater wireless networks, IEEE J. Ocean. Eng. 35 (3) (2010) 623–634.
- [57] P. Xie, J.-H. Cui, An FEC-based reliable data transport protocol for underwater sensor networks, in: Proc. of IEEE ICCCN, Honolulu, HI, 2007.
- [58] L. Lu, L. Zhong, Energy and time efficient topology control algorithm for underwater acoustic ad hoc networks, in: Proc. of ICCET, Chengdu, China, 2010.
- [59] M. Stojanovic, On the relationship between capacity and distance in an underwater acoustic communication channel, ACM Mobile Comput. and Commun. Review 11 (4) (2007) 34–43.
- [60] C. Schurgers, V. Tsiatsis, S. Ganeriwal, M. B. Srivastava, Optimizing Sensor Networks in the Energy-Latency-Density Design Space, IEEE Trans. Mobile Comput. 1 (1) (2002) 70–80.
- [61] M. J. Miller, N. H. Vaidya, A MAC protocol to reduce sensor network energy consumption using a wakeup radio, IEEE Trans. Mobile Comput. 4 (3) (2005) 228–242.
- [62] L. Freitag, M. Grund, S. Singh, J. Partan, P. Koski, K. Ball, The WHOI micro-modem: An acoustic communications and navigation system for multiple platforms, <http://acomms.who.edu/umodem/> (2005).
- [63] Teledyne-Benthos Acoustic Modems.
URL <http://www.benthos.com/acoustic-teleonar-modem-product-comparison.asp>
- [64] A. Syed, M. O. Khan, J. Heidemann, J. Wills, W. Ye, A sensor-net-inspired underwater acoustic modem for wake-up and data (demo abstract), in: Proc. of ACM WUWNet, San Francisco, CA, 2008.
- [65] M. Zorzi, R. R. Rao, Geographic random forwarding (GeRaF) for ad hoc and sensor networks: multihop performance, IEEE Trans. Mobile Comput. 2 (4) (2003) 337–348.
- [66] F. J. Millero, A. Poisson, C. T. Chen, A. L. Bradshaw, K. Schleicher, Background papers and supporting data on the International Equation of State of Seawater, UNESCO technical papers in marine science.
URL <http://unesdoc.unesco.org/images/0004/000473/047363eb.pdf>
- [67] B. D. Dushaw, P. F. Worcester, B. D. Cornuelle, B. M. Howe, On equations for the speed of sound in seawater, J. Acoust. Soc. Am. 93 (1) (1993) 255–275.
- [68] K. V. Mackenzie, Nine-term equation for the sound speed in the oceans, J. Acoust. Soc. Am. 70 (3) (1981) 807–812.
- [69] V. A. Del Grosso, New equation for speed of sound in natural waters, J. Acoust. Soc. Am. 56 (4) (1974) 1084–1091.
- [70] C. S. Meinen, D. R. Watts, Further evidence that the sound-speed algorithm of Del Grosso is more accurate than

- that of Chen and Millero, *J. Acoust. Soc. Am.* 102 (4) (1997) 2058–2062.
- [71] M. Porter *et al.*, Bellhop code.
URL <http://oalib.hlsresearch.com/Rays/index.html>
- [72] F. Jensen, W. Kuperman, M. Porter, H. Schmidt, *Computational Ocean Acoustics*, 2nd Edition, Springer-Verlag, New York, 1984, 2nd printing 2000.
- [73] World ocean simulation system web site.
URL <http://telecom.dei.unipd.it/ns/woss>
- [74] N. Baldo, M. Miozzo, F. Guerra, M. Rossi, M. Zorzi, MIRACLE: The Multi-Interface Cross-Layer Extension of ns2, *EURASIP Journal on Wireless Communications and Networking*.
URL <http://www.hindawi.com/journals/wcn/2010/761792/cta/>
- [75] World Ocean Atlas.
URL www.nodc.noaa.gov/OC5/WOA05/pr_woa05.html
- [76] General Bathymetric Chart of the Oceans.
URL www.gebco.net
- [77] National Geophysical Data Center, seafloor surficial sediment descriptions.
URL <http://www.ngdc.noaa.gov/mgg/geology/deck41.html>
- [78] L. D. Hampton, Acoustic properties of sediments, *J. Acoust. Soc. Am.* 42 (1967) 882–890.
- [79] E. L. Hamilton, Sound velocity-density relations in sea-floor sediments and rocks, *J. Acoust. Soc. Am.* 63 (1978) 366–377.
- [80] E. L. Hamilton, Geoacoustic modeling of the sea floor, *J. Acoust. Soc. Am.* 68 (1980) 1313–1340.
- [81] P. Milholland, M. H. Manghnani, S. O. Schlanger, G. H. Sutton, Geoacoustic modeling of deep-sea carbonate sediments, *J. Acoust. Soc. Am.* 68 (1980) 1351–1360.
- [82] F. A. Bowles, Observations on attenuation and shear-wave velocity in fine-grained, marine sediments, *J. Acoust. Soc. Am.* 101 (1997) 3385–3397.
- [83] M. Siderius, J.-P. Hermand, Yellow shark spring 1995: Inversion results from sparse broadband acoustic measurements over a highly range-dependent soft clay layer, *J. Acoust. Soc. Am.* 106 (1999) 637–651.
- [84] F. Guerra, P. Casari, A. Berni, J. R. Potter, M. Zorzi, Performance evaluation of random and handshake-based channel access in collaborative mobile underwater networks, in: *Proc. of MTS/IEEE Oceans*, Seattle, WA, 2010.
- [85] J. Shusta, Acoustic network architecture (demo abstract), in: *Proc. of ACM WUWNet*, Woods Hole, MA, 2010.
- [86] M. Rossi, N. Bui, G. Zanca, L. Stabellini, R. Crepaldi, M. Zorzi, SYNAPSE++: Code dissemination in wireless sensor networks using fountain codes, *IEEE Trans. Mobile Comput.* 9 (12) (2010) 1749–1765.
- [87] P. Levis, N. Patel, D. E. Culler, S. Shenker, Trickle: A self-regulating algorithm for code propagation and maintenance in wireless sensor networks., in: *NSDI, USENIX*, 2004, pp. 15–28.
- [88] Evologics S2C series modems.

URL <http://www.evologics.de/en/products/acoustics/index.html>

- [89] E. M. Sozer, M. Stojanovic, Reconfigurable acoustic modem for underwater sensor networks, in: Proc. of ACM WUWNet, Los Angeles, CA, 2006.
- [90] M. Aydinlik, A. T. Ozdemir, M. Stojanovic, A physical layer implementation on reconfigurable underwater acoustic modem, in: Proc. of MTS/IEEE Oceans, Québec City, Canada, 2008.
- [91] I. Vasilescu, C. Detweiler, D. Rus, AquaNodes: An underwater sensor network, in: Proc. of MTS/IEEE Oceans, Montréal, Canada, 2007.
- [92] D. Torres, J. Friedman, T. Schmid, M. B. Srivastava, Software-defined underwater acoustic networking platform, in: Proc. of ACM WUWNet, Montréal, Canada, 2007.
- [93] W. S. Hodgkiss, J. D. Skinner, A multichannel software-defined acoustic modem, in: Proc. of ECUA, Istanbul, Turkey, 2010.
- [94] Aquatec Group.
URL <http://www.aquatecgroup.com/>
- [95] Develogic subsea systems.
URL <http://www.develogic.de/>
- [96] L3 ELAC Nautik.
URL <http://www.elac-nautik.de/>
- [97] Sonardyne Acoustic Modems.
URL <http://www.sonardyne.de/>

Name (Manufacturer)	Frequency band	Modulation	Data rate	Power (TX, RX/Idle, Sleep)	Range	BER ^d
Commercial modems						
AquaModem (Aquatec) [94]	8–16 kHz	DSSS or MFSK	300–2000 bps	20 W, 0.6 W, 5 mW	Up to 20 km	10 ⁻⁶
HAMNode (Develogic) [95]	3–6 to 40–85 kHz	OFDM–MDFSK	3.4–7 kbps	80 W, 3 W, 1 mW ^b	Up to 30 km	N/A
S2C series (Evologics) [88]	18–34 or 48–78 kHz	S2C ^c MFSK	Up to 20 kbps	100 W, 0.8 W, 8 mW ^b	Up to 6 km	10 ⁻⁶
UM30 (ELAC Nautik) [96]	10–14 kHz or 25–35 kHz	MFSK	Up to 3840 bps	100 W, 3 W, 10 mW	N/A	10 ⁻³
uCOMM (Sonarbyte) [97]	14–22 kHz or 19–36 kHz	QPSK	1.5–15 kbps	50 W, 1 W, 30 mW	Up to 7 km	10 ⁻⁸
ATM-886 (Teledyne Benthos)	9–14 kHz or 16–21 kHz	MFSK, PSK	Up to 15 kbps	N/A	Up to 6 km	10 ⁻⁷
UWM2000 (Linkquest)	27–45 kHz	N/A	6.6 kbps	8 W, 0.8 W, 8 mW	1.2 km	10 ⁻⁹
Research modems						
μ Modem (WHOI) [62]	4-kHz band from 3 to 30 kHz	FH–BFSK, MPSK	Up to 5400 bps	50 W, 2 W, 40 mW ^b	Up to 9 km	N/A
rModem (MIT) [90]	1–100 kHz	QPSK	550 bps	N/A	Tested at 100 m	N/A
AquaNode (MIT) [91]	Around 30 kHz	FSK	330 bps	N/A	400 m	N/A
MIMO-OFDM (UComm) [8]	N/A	QPSK, QAM	Up to 125.7 kbps	N/A	N/A	N/A
UANT (UCLA) [92]	0–50 MHz ^d	GMSK	From 244 bps to 500 kbps	N/A	N/A	N/A
Low cost (UCSD) ^e [7]	32–38 kHz	FSK	200 bps	40 W, 1 W, N/A ^b	2 km	10 ⁻²
SDAM (Scriptps) [93]	10–32 kHz	PWM	100 kbps	150 W, 20 W, 2.5 W	N/A	N/A
SNUSE modem (USC) [64]	17–19 kHz	FSK	1 kbps ^b	N/A	< 500 m	N/A

^a This data is usually measured in the high SNR region. For the UCSD modem [7], it has been measured at an SNR of 10 dB.

^b Maximum values.

^c Sweep-spread carrier technique.

^d This parameter is what is reported in [92] and is due to the GNURadio specifications. For acoustic communications, it would have to be set to a more feasible value.

^e The modem is currently at an advanced design stage.

Table 2: Summary of the features of some commercial and research modems: operating frequency band, modulation, data rate, power consumption, declared coverage range and bit error rate (BER).